# A Unique Matched Quadruplet of Terbium Radioisotopes for PET and SPECT and for α- and β⁻-Radionuclide Therapy: An In Vivo Proof-of-Concept Study with a New Receptor-Targeted Folate Derivative

Cristina Müller*[1], Konstantin Zhernosekov*[1,2], Ulli Köster[3], Karl Johnston[4], Holger Dorrer[2,5], Alexander Hohn[1], Nico T. van der Walt[6], Andreas Türler[2,5], and Roger Schibli[1,7]

*[1]Center for Radiopharmaceutical Sciences ETH-PSI-USZ, Paul Scherrer Institute, Villigen-PSI, Switzerland; [2]Laboratory of Radiochemistry and Environmental Chemistry, Paul Scherrer Institute, Villigen-PSI, Switzerland; [3]Institut Laue-Langevin, Grenoble, France; [4]Physics Department, ISOLDE/CERN, Geneva, Switzerland; [5]Department of Chemistry and Biochemistry, Laboratory of Radiochemistry and Environmental Chemistry, University of Bern, Bern, Switzerland; [6]Faculty of Applied Sciences, Cape Peninsula University of Technology, Bellville, South Africa; and [7]Department of Chemistry and Applied Biosciences, ETH Zurich, Zurich, Switzerland*

Terbium offers 4 clinically interesting radioisotopes with complementary physical decay characteristics: $^{149}$Tb, $^{152}$Tb, $^{155}$Tb, and $^{161}$Tb. The identical chemical characteristics of these radioisotopes allow the preparation of radiopharmaceuticals with identical pharmacokinetics useful for PET ($^{152}$Tb) and SPECT diagnosis ($^{155}$Tb) and for α- ($^{149}$Tb) and β⁻-particle ($^{161}$Tb) therapy. The goal of this proof-of-concept study was to produce all 4 terbium radioisotopes and assess their diagnostic and therapeutic features in vivo when labeled with a folate-based targeting agent. **Methods:** $^{161}$Tb was produced by irradiation of $^{160}$Gd targets with neutrons at Paul Scherrer Institute or Institut Laue-Langevin. After neutron capture, the short-lived $^{161}$Gd decays to $^{161}$Tb. $^{149}$Tb, $^{152}$Tb, and $^{155}$Tb were produced by proton-induced spallation of tantalum targets, followed by an online isotope separation process at ISOLDE/CERN. The isotopes were purified by means of cation exchange chromatography. For the in vivo studies, we used the DOTA–folate conjugate cm09, which binds to folate receptor (FR)–positive KB tumor cells. Therapy experiments with $^{149}$Tb-cm09 and $^{161}$Tb-cm09 were performed in KB tumor–bearing nude mice. Diagnostic PET/CT ($^{152}$Tb-cm09) and SPECT/CT ($^{155}$Tb-cm09 and $^{161}$Tb-cm09) studies were performed in the same tumor mouse model. **Results:** Carrier-free terbium radioisotopes were obtained after purification, with activities ranging from approximately 6 MBq (for $^{149}$Tb) to approximately 15 GBq (for $^{161}$Tb). The radiolabeling of cm09 was achieved in a greater than 96% radiochemical yield for all terbium radioisotopes. Biodistribution studies showed high and specific uptake in FR-positive tumor xenografts (23.8% ± 2.5% at 4 h after injection, 22.0% ± 4.4% at 24 h after injection, and 18.4% ± 1.8% at 48 h after injection). Excellent tumor-to-background ratios at 24 h after injection (tumor to blood, ~15; tumor to liver, ~5.9; and tumor to kidney, ~0.8) allowed the visualization of tumors in mice using PET ($^{152}$Tb-cm09) and SPECT ($^{155}$Tb-cm09 and $^{161}$Tb-cm09). Compared with no therapy, α- ($^{149}$Tb-cm09) and β⁻-particle therapy ($^{161}$Tb-cm09) resulted in a marked delay in tumor growth or even complete remission (33% for $^{149}$Tb-cm09 and 80% for $^{161}$Tb-cm09) and a significantly increased survival. **Conclusion:** For the first time, to our knowledge, 4 terbium radionuclides have been tested in parallel with tumor-bearing mice using an FR targeting agent. Along with excellent tumor visualization enabled by $^{152}$Tb PET and $^{155}$Tb SPECT, we demonstrated the therapeutic efficacy of the α-emitter $^{149}$Tb and β⁻-emitter $^{161}$Tb.

**Key Words:** terbium radioisotopes; folate receptor targeting; SPECT; PET; radionuclide therapy

**J Nucl Med 2012; 53:1951–1959**
DOI: 10.2967/jnumed.112.107540

Because of its physical half-lives ($T_{1/2}$), decay properties, and energies, the lanthanide terbium is one of the few elements that features 4 clinically interesting radioisotopes (Table 1). $^{149}$Tb has a half-life of 4.12 h and emits short-range α-particles at an energy ($E_\alpha$) of 3.967 MeV with an intensity of 17%. It is the only α-emitter among radiolanthanides with a suitable half-life for application in radionuclide therapy. $^{152}$Tb ($T_{1/2}$, 17.5 h) emits positrons of an average energy of 1.080 MeV with an intensity of 17%. The radionuclide would be useful for patient-specific dosimetry using PET before the application of therapeutic radiolanthanides. $^{155}$Tb ($T_{1/2}$, 5.32 d) decays by electron capture (EC) and emits γ-rays of 86.55 keV (32%) and 105.3 keV (25%). $^{155}$Tb could be used for SPECT without adding a high radiation dose burden to the patient. $^{161}$Tb emits low-energy β⁻-particles of an average energy ($E_{\beta^- \text{ average}}$) of 0.154 MeV and with an intensity of 100%. In addition, it emits also Auger electrons and

Received Apr. 17, 2012; revision accepted Jul. 2, 2012.
For correspondence or reprints contact: Roger Schibli, Center for Radiopharmaceutical Sciences ETH-PSI-USZ, Paul Scherrer Institute, 5232 Villigen-PSI, Switzerland.
E-mail: roger.schibli@psi.ch
*Contributed equally to this work.
Published online Nov. 8, 2012.
COPYRIGHT © 2012 by the Society of Nuclear Medicine and Molecular Imaging, Inc.



UH & EURATOM Exhibit 2041-001
Fusion v. Universität Heidelberg, et al.
IPR2023-00551

**TABLE 1**
Decay Characteristics of Terbium Radionuclides Useful for Medical Application (Main γ-Lines Are Given)

| Nuclide | Decay mode and branching | $T_{1/2}$ | $E_\alpha$ (MeV) | $E_{\beta av}$ (MeV) | $E_\gamma$ (keV) | $I_\gamma$ (%) | Application |
|---|---|---|---|---|---|---|---|
| $^{149}$Tb | α (16.7%), $\beta^+$ (7.1%) | 4.12 h | 3.967 | 0.730 | 165.0 | 26 | α-therapy |
| | | | | | 352.2 | 29 | |
| | | | | | 388.6 | 18 | |
| | | | | | 652.1 | 16 | |
| $^{152}$Tb | $\beta^+$ (17%) | 17.5 h | — | 1.080 | 271.1 | 8.6 | PET |
| | | | | | 344.3 | 65 | |
| | | | | | 586.3 | 9.4 | |
| | | | | | 778.9 | 5.8 | |
| $^{155}$Tb | EC (100%) | 5.32 d | — | — | 86.55 | 32 | SPECT |
| | | | | | 105.3 | 25 | |
| | | | | | 180.1 | 7.5 | |
| | | | | | 262.3 | 5.3 | |
| $^{161}$Tb | $\beta^-$ (100%) | 6.89 d | — | 0.154 | 25.65 | 23 | $\beta^-$-/Auger therapy |
| | | | | | 48.92 | 17 | |
| | | | | | 57.19 | 1.8 | |
| | | | | | 74.57 | 10 | |

γ-radiation (48.92 keV [17%], 57.19 keV [1.8%], and 74.57 keV [10%]) suitable for SPECT.

Beyer et al. reported promising therapeutic results for $^{149}$Tb-labeled rituximab in a mouse model carrying human xenografts expressing the CD20 antigen (*1*). The same group has proposed $^{152}$Tb as a radioisotope for kinetics studies with PET (*2*). Our group has recently reported an efficient production route for $^{161}$Tb that could be a better alternative to the clinically used $^{177}$Lu (*3*). Thus, these 4 radionuclides of one and the same element are suitable for all modalities of nuclear imaging and radionuclide therapy, featuring identical chemical characteristics and ultimately identical pharmacologic characteristics of the corresponding radioconjugates.

The vitamin folic acid has successfully been used as a targeting ligand for the selective delivery of attached probes to folate receptor (FR)–positive cancer cells (*4–6*). For a proof of concept of the utility of these 4 radionuclides, we took advantage of a recently developed novel DOTA–folate conjugate comprising an albumin-binding entity (cm09) (Fig. 1).

This folate conjugate has been successfully used for targeting of the tumor-associated FR in preclinical studies (*7*). Because of its extended blood circulation, as a consequence of its plasma protein binding, the biologic half-life of cm09 matches well with the physical half-lives of the longer-lived terbium-radioisotopes.

Herein, we report the first, to our knowledge, in vitro and in vivo study with 4 terbium radionuclides. They have been investigated with the same targeting molecule—a novel FR-targeting folate derivative cm09—and an identical tumor model for their applicability for PET and SPECT as well as for targeted α- and $\beta^-$-radionuclide therapy in FR-positive tumor-bearing mice.

## MATERIALS AND METHODS

### Production of $^{149}$Tb, $^{152}$Tb, and $^{155}$Tb

$^{149}$Tb, $^{152}$Tb, and $^{155}$Tb were produced by high-energy proton-induced spallation of tantalum foil targets. The spallation products were released from the hot target ionized by a surface ionization source and mass separated at the online isotope separator ISOLDE (CERN). The ionized products were separated according to their mass-to-charge ratio as previously reported by Allen et al. (*2,8*). The spallation products of mass numbers 149, 152, and 155 were collected on a zinc-coated gold foil. After dissolution of the zinc layer in 0.1 M HCl, the terbium radioisotopes were separated from isobar and pseudoisobar impurities and stable zinc. Cation exchange chromatography was performed using a self-made column (dimensions, 50 × 5 mm) filled with a strongly acidic cation exchanger similar to that previously described (*2,3*). A solution of α-hydroxyisobutyric acid adjusted with ammonia to pH 4.75 was used as an elution agent. To avoid time-consuming additional steps for preconcentration by evaporation and therefore to minimize loss of radioactivity, the fractions of terbium radioisotopes (obtained in less than 1 mL of α-hydroxyisobutyrate solution [~0.15 M]) were directly used for radiolabeling of the folate conjugate (cm09).

### Production of $^{161}$Tb

The production of no-carrier-added $^{161}$Tb was recently reported by Lehenberger et al. (*3*). Briefly, highly enriched $^{160}$Gd targets were irradiated during 2–3 wk at the spallation-induced neutron

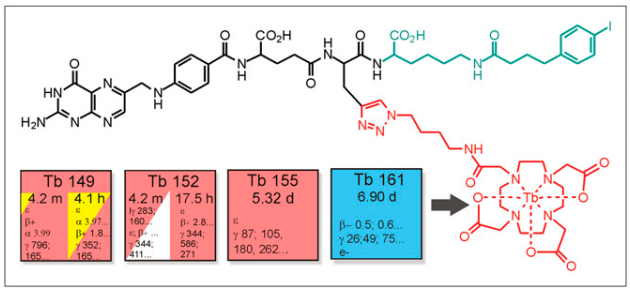


**FIGURE 1.** Chemical structure of terbium-cm09 comprising 3 functionalities: black indicates folic acid as targeting agent; green, albumin-binding entity to prolong blood circulation time; and red, terbium radioisotope stably coordinated by a DOTA chelator. Tb = terbium.



UH & EURATOM Exhibit 2041-002
Fusion v. Universität Heidelberg, et al.
IPR2023-00551

source SINQ at Paul Scherrer Institute (PSI) or during 1 wk at the high-flux nuclear reactor at the Institut Laue-Langevin (ILL). Isolation of $^{161}$Tb was performed at PSI by means of cation exchange chromatography (*3*). $^{161}$Tb was formulated in a solution of 200–300 μL of HCl 0.05 M.

### Radiofolate Synthesis

A $^{161}TbCl_3$ solution (7 μL, 200 MBq) was added to a mixture of cm09 (5 μL, $10^{-3}$ M), HCl (0.05 M, 43 μL), and sodium acetate (10 μL, 0.5 M). The reaction solution was heated for 15 min at 95°C. Na-diethylenetriaminepentaacetic acid (10 μL, 5 mM, pH 5) was added, and quality control was performed by means of high-performance liquid chromatography (HPLC) (supplemental data; available online only at http://jnm.snmjournals.org). The mobile phase consisted of an aqueous 0.05 M triethylammonium phosphate buffer (pH 2.25) (A) and methanol (B) with a linear gradient from 5% B to 80% B over 25 min and a flow rate of 1 mL/min. The retention time of terbium-cm09 was approximately 19.7 min, whereas traces of unreacted Tb(III)-diethylenetriaminepentaacetic acid were determined at 3.2–3.6 min. $^{161}$Tb-cm09 was obtained with a specific activity of up to 40 MBq/nmol and a radiochemical yield of greater than 98%. High-performance liquid chromatograms are shown in the supplemental data. For biodistribution and SPECT studies, $^{161}$Tb-cm09 was used at specific activities of approximately 6.0 MBq/nmol and approximately 27.0 MBq/nmol, respectively. For therapeutic application, $^{161}$Tb-cm09 was prepared at a specific activity of approximately 2.75 MBq/nmol.

For PET studies, about 20 MBq of $^{152}$Tb in α-hydroxyisobutyrate (0.15 M, pH 4.75, 500 μL) were directly added to a vial containing cm09 (15 μL, $10^{-3}$ M). For SPECT studies, about 4.5 MBq of $^{155}$Tb in α-hydroxyisobutyrate (0.15 M, pH 4.75, 300 μL) were directly added to a vial containing cm09 (7 μL, $10^{-3}$ M). Subsequent reaction steps were performed as described for the preparation of $^{161}$Tb-cm09. Quality control revealed a greater than 96% radiochemical yield of $^{152}$Tb-cm09 at a specific activity of approximately 1.33 MBq/nmol and a greater than 96% radiochemical yield of $^{155}$Tb-cm09 at a specific activity of approximately 0.64 MBq/nmol (supplemental data). About 5.8 MBq of $^{149}$Tb in α-hydroxyisobutyrate (0.15 M, pH 4.75, 700 μL) were directly added to a vial containing cm09 (12 μL, $10^{-3}$ M) using the same reaction steps as reported for $^{161}$Tb-cm09. The product $^{149}$Tb-cm09 was obtained in a greater than 96% radiochemical yield at a specific activity of approximately 0.48 MBq/nmol (supplemental data). For in vivo application of $^{149/152/155}$Tb-cm09, a solution of NaCl 9% (~0.05 μL per 100 μL) was added to the labeling solution to increase the osmolarity to a physiologic value of 280 mOsm/L.

### In Vitro Evaluation

Because of the easy availability and high radiochemical yield, the in vitro analysis and optimization have been performed with $^{161}$Tb.

The potential radiolysis of $^{161}$Tb-cm09 was investigated by incubation of $^{161}$Tb-cm09 (80 MBq, 2 nmol) in 400 μL of phosphate-buffered saline (PBS), pH 7.4. Samples were taken at 1, 2, 4, 24, and 48 h after incubation and analyzed using HPLC. To investigate the radioconjugate's stability, $^{161}$Tb-cm09 (50 μL, ~1.5 MBq) was incubated in human plasma (250 μL) at 37°C. Aliquots of plasma (50 μL) were taken at different time points up to 168 h. After precipitation of the proteins by the addition of 200 μL of methanol, supernatants were analyzed using HPLC. The distribution coefficient (LogD value) in octanol and PBS, pH 7.4, were determined according to a standard protocol, which has previously been applied for other folate radioconjugates (*9*).

### Cell Experiments

Cell experiments were performed with $^{161}$Tb-radiolabeled cm09, KB cells (human cervical carcinoma cell line, HeLa subclone; ACC-136) were purchased from the German Collection of Microorganisms and Cell Cultures (DSMZ). The cells were cultured as monolayers at 37°C in a humidified atmosphere containing 5% $CO_2$ using a folate-free cell culture medium, FFRPMI (modified RPMI, without folic acid, vitamin $B_{12}$, and phenol red; Cell Culture Technologies GmbH). FFRPMI medium was supplemented with 10% heat-inactivated fetal calf serum (as the only source of folate), L-glutamine, and antibiotics (penicillin–streptomycin–fungizone).

KB cells were seeded in 12-well plates to grow overnight (~700,000 cells in 2 mL of FFRPMI medium per well). HPLC-purified $^{161}$Tb-cm09 (~38 kBq, 8 pmol) was added to each well. In some wells, an excess of folic acid (100 μM) was added to block FRs on the cellular surface. After incubation for 2 and 4 h at 37°C, the cells were washed with PBS to determine total uptake of the radioconjugate. To assess the internalized fraction of $^{161}$Tb-cm09, KB cells were washed with an acidic stripping buffer (*10*) to release FR-bound radioconjugates from the cell surface. Cell lysis was accomplished by adding 1 mL of NaOH (1 M) to each well. The cell suspensions were transferred to 4-mL tubes for measurement in a γ-counter. After homogenization in a vortex mixer, the concentration of proteins was determined for each sample by a Micro BCA Protein Assay kit (Pierce, Thermo Scientific) to standardize measured radioactivity to the average content of 0.3 mg of protein in a single well.

### Biodistribution Studies

In vivo experiments were approved by the local veterinary department and conducted in accordance with the Swiss law of animal protection. Six- to 8-wk-old female athymic nude mice (CD-1 Foxn-1/nu) were purchased from Charles River Laboratories. The animals were fed with a folate-deficient rodent diet (Harlan Laboratories) starting 5 d before the tumor cell inoculation (*11*). Mice were inoculated with KB cells ($5 \times 10^6$ cells in 100 μL of PBS) into the subcutis of each shoulder, and biodistribution studies were performed approximately 14 d later. $^{161}$Tb-cm09 was diluted in PBS, pH 7.4 (~3 MBq, 0.5 nmol per mouse), for immediate administration via a lateral tail vein. At 1, 4, 24, 48, 96, and 168 h after the administration of $^{161}$Tb-cm09, the mice were euthanized and dissected. Selected tissues and organs were collected, weighed, and counted for radioactivity in a γ-counter. The results were listed as percentage of the injected dose per gram of tissue weight (%ID/g), using reference counts from a definite sample of the original injectate that was counted at the same time. Dosimetric calculations are reported in the supplemental data.

### PET and SPECT Studies

SPECT scans were obtained using a dedicated small-animal SPECT/CT scanner (X-SPECT system; Gamma-Medica Inc.). The detector was equipped with a 1-mm tungsten-based single-pinhole collimator. PET scans were acquired with a dedicated small-animal PET/CT scanner (Vista eXplore; GE Healthcare).

*Phantom Images.* Derenzo phantoms with hole diameters ranging from 0.8 to 1.3 mm, in 0.1-mm steps, were filled with approximately 50 MBq of $^{161}$Tb and approximately 0.6 MBq of



UH & EURATOM Exhibit 2041-003
Fusion v. Universität Heidelberg, et al.
IPR2023-00551

$^{155}$Tb solutions for SPECT. The 74.57-keV ($^{161}$Tb) and 86.55- and 105.3-keV ($^{155}$Tb) γ-lines were used for reconstruction. For PET, the phantom was filled with approximately 1.9 MBq of $^{152}$Tb.

*In Vivo Imaging.* Imaging studies were performed with KB tumor–bearing mice approximately 14 d after tumor cell inoculation. $^{152}$Tb-cm09 (~9 MBq, ~6.8 nmol per mouse) was injected intravenously in 2 mice. PET scans lasting 90 min were obtained for each of these mice at 1.5 and 3 h after injection. The mouse that was scanned at 3 h after injection of $^{152}$Tb-cm09 was euthanized the following day and rescanned post mortem for 4 h. All PET scans were followed by a CT scan. PET and CT data were reconstructed with the instrument's software. For PET reconstruction, the 2-dimensional ordered-subset expectation maximization algorithm was used. PET and CT data were fused using PMOD software (version 3.3; PMOD Technologies Ltd.). Parts of the PET studies are reported in the supplemental data.

$^{155}$Tb-cm09 (~4 MBq; ~6.3 nmol) was injected intravenously. An in vivo scan lasting 1 h was obtained at 24 h after injection of $^{155}$Tb-cm09. A post mortem 2-h SPECT scan was acquired at 4 d after injection of $^{155}$Tb-cm09. An in vivo SPECT scan of 15 min was obtained at 24 h after intravenous injection of $^{161}$Tb-cm09 (~30 MBq; ~1.1 nmol). All SPECT scans were followed by a CT scan. SPECT data were acquired and reconstructed using LumaGEM software (version 5.407; Gamma-Medica Inc.). CT data were acquired with an x-ray CT system (Gamma-Medica Inc.) and reconstructed with COBRA (version 4.5.1; Exxim-Computing Corp.). SPECT and CT data were fused using an application in an IDL Virtual Machine environment (version 6.0; ITT Visual Information Solutions). All images (PET and SPECT) were generated by Amira software (version 4.0.1; Mercury Computer Systems). Parts of the SPECT studies are reported in the supplemental data.

### In Vivo Therapy Studies with $^{149}$Tb-cm09 and $^{161}$Tb-cm09

Mice were inoculated with KB tumor cells ($4.5 \times 10^6$ cells in 100 μL of PBS) on each shoulder 4 d before the start of therapy. For the study with $^{149}$Tb-cm09, 2 groups of 3 mice were injected with only PBS (group a: control) or with the available amount of $^{149}$Tb-cm09 (group b: day 0, 1.1 MBq; and day 4, 1.3 MBq, ~4 nmol). At day 0 (first injection), the average tumor volume reached 93 mm$^3$ for group a and 83 mm$^3$ for group b. At day 4 (second injection), the average tumor volume reached 156 mm$^3$ for group a and 110 mm$^3$ for group b.

The study with $^{161}$Tb-cm09 was designed according to the parameters applied for the study with $^{149}$Tb-cm09. Two groups of 5 mice each were injected either with only PBS (group c: control) or with $^{161}$Tb-cm09 (group d: 11 MBq, ~4 nmol). At the day of injection, the average tumor volumes reached values of 128 mm$^3$ for group c and 125 mm$^3$ for group d.

Endpoint criteria were defined as weight loss of more than 15% of the initial body weight, single tumor volume (right or left) greater than 1,500 mm$^3$, active ulceration of the tumor, or abnormal behavior indicating pain or unease. Tumor volume and body weight were determined at day 0 (i.e., the first day of radioconjugate administration) and then every other day until the completion of the study at day 56. Tumor measurement was performed using a digital caliper. The tumor size was calculated using the formula ($0.5 \times$ [length $\times$ width$^2$]). Mice were removed from the study and euthanized on reaching one of the predefined endpoint criteria. To calculate the significance of the survival time, a *t* test was used. All analyses were 2-tailed and considered as type 3 (2-sample unequal variance). A *P* value of less than 0.05 was considered statistically significant.

## RESULTS

### Production of Terbium Radioisotopes

The ISOLDE facility at CERN allowed access to carrier-free $^{149/152/155}$Tb radioisotopes. After transport to PSI and radiochemical processing by a 1-step separation method based on cation exchange chromatography, activities of approximately 5.8 MBq of $^{149}$Tb, approximately 18 MBq of $^{152}$Tb, and approximately 11 MBq of $^{155}$Tb were available. The radionuclides were obtained in a small volume of α-hydroxyisobutyrate solution (pH 4.75). Because the α-hydroxyisobutyrate solution is useful as a buffer system (p$K_a$, 3.97), it can be directly used for performance of the radiolabeling reaction. $^{161}$Tb was produced by neutron irradiation of highly enriched $^{160}$Gd at the neutron source SINQ at PSI or at the nuclear high-flux reactor at the ILL. After cation exchange chromatography performed according to a previously described procedure (*3*), this radionuclide was obtained at an activity of approximately 15 GBq in a small volume of diluted hydrochloric acid solution with chemical purity suitable for radiolabeling reactions.

### Radiolabeling and Stability Experiments

The folate conjugate (cm09) was radiolabeled with $^{161}$Tb according to a standard procedure at pH 4.5. To achieve quantitative incorporation of the radioisotope, the reaction vial was heated at 95°C for 15 min. In contrast, cm09 was radiolabeled with $^{149}$Tb, $^{152}$Tb, and $^{155}$Tb directly in the chromatography's elution agent, α-hydroxyisobutyrate solution (pH 4.75), to minimize the overall expenditure of time and therefore loss of radioactivity. Quality control revealed a radiochemical yield of greater than 96% for all terbium-cm09 radioconjugates. Results of HPLC analysis are shown in the supplemental data. Experiments performed with high amounts of radioactivity incubated in a small volume of PBS at room temperature revealed an excellent stability of $^{161}$Tb-cm09. Decomposition of $^{161}$Tb-cm09 as a consequence of radiolysis was not observed during the first 4 h of incubation. Only a small amount of a radioactive side-product (retention time, 17.6 min; ~5% integrated peak area) of unknown composition was found after 24 h, which was slightly increased (~7%) after 48 h. Free Tb (III) was not detected by HPLC analysis over the whole period of investigation. In human plasma, $^{161}$Tb-cm09 was completely stable over a period of 168 h.

### In Vitro and In Vivo Characterization of $^{161}$Tb-cm09

In vitro and post mortem biodistribution studies have been performed exclusively with $^{161}$Tb-cm09 because of the availability of this isotope. In vitro cell uptake studies with FR-positive KB cells showed a high uptake of $^{161}$Tb-cm09 after an incubation period of 2 and 4 h (Fig. 2). The internalized fraction was about 30% of total cell-bound $^{161}$Tb-cm09. FR-specific binding was proven by experiments with excess folic acid, resulting in an almost complete decline (<1%) of $^{161}$Tb-cm09 uptake.



UH & EURATOM Exhibit 2041-004
Fusion v. Universität Heidelberg, et al.
IPR2023-00551

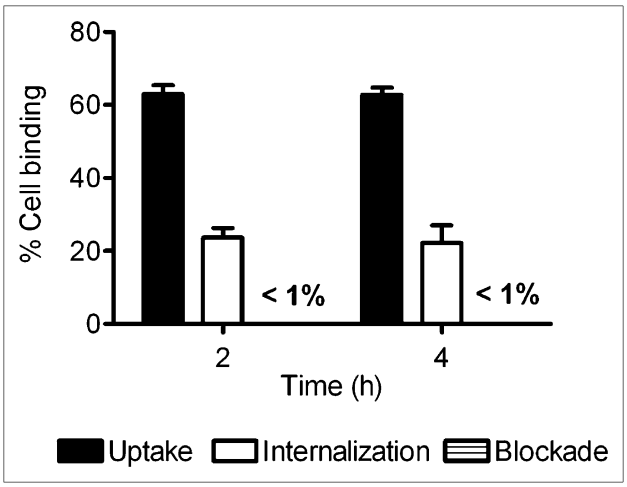


**FIGURE 2.** Cell uptake and internalization of $^{161}$Tb-cm09 in FR-positive KB tumor cells after incubation at 37°C. Blockade of FRs by preincubation of cells with excess folic acid reduced FR binding of $^{161}$Tb-cm09 to less than 1%.

Biodistribution studies were performed with $^{161}$Tb-cm09 over a period of 7 d (Table 2). Uptake of radioactivity in tumor xenografts was already high shortly after injection (14.1 ± 0.6 %ID/g, 1 h after injection) and increased over time up to 23.8 ± 2.5 %ID/g at 24 h after injection. Washout of radioactivity from the tumor tissue was slow, resulting in respectable amounts of radioactivity (5.7 ± 1.9 %ID/g) even 7 d after injection of $^{161}$Tb-cm09. Undesired uptake and retention of $^{161}$Tb-cm09 was found only in the kidneys. Twenty-four hours after injection, high tumor-to-background ratios were achieved (tumor to blood, ~15; tumor to liver, ~5.9; and tumor to kidney, ~0.8), allowing excellent target–to–non-target contrast for imaging purposes via SPECT (Fig. 3). The results of dosimetric calculations are reported in the supplemental data.

### PET and SPECT In Vitro and In Vivo Imaging

Derenzo phantom PET measurements of $^{152}$Tb revealed relatively poor spatial resolution (Fig. 3A), most likely a result of the high positron energy of $^{152}$Tb and the presence of additional γ-rays. However, 24 h after injection of $^{152}$Tb-cm09 excellent images were obtained, allowing a clear visualization of tumor xenografts and kidneys (Fig. 3D; supplemental data). In background organs and tissues, the accumulation of radioactivity was largely absent.

High-quality imaging of Derenzo phantoms was possible by means of SPECT with the photon-emitting terbium isotopes $^{155}$Tb and $^{161}$Tb. Apart from $\beta^-$-particles and Auger electrons, $^{161}$Tb also emits γ-radiation. The γ-ray (energy, 74.57 keV; intensity, 10%) was used for SPECT (Figs. 3B and 3C). In vivo application of $^{155}$Tb-cm09 and $^{161}$Tb-cm09 allowed excellent tumor visualization at 24 h after injection (Figs. 3E and 3F). The relatively long half-life of $^{155}$Tb allowed longitudinal imaging, as demonstrated by a SPECT/CT scan obtained at 4 d after injection (supplemental data).

### Targeted α- and $\beta^-$-Radionuclide Therapy

The set-up of the therapy studies is shown in Table 3. Because $^{149}$Tb was not readily available, only a limited number of tumor-bearing mice could be included in this therapy study. Despite the possibility of preparing $^{161}$Tb-cm09 at significantly higher specific activities (≥40 MBq/nmol), it was administered at a low specific activity to approximate the molar amount of cm09 (~4 nmol) injected per mouse for both therapy experiments. Although tumors grew quickly in mice injected only with PBS (group a), a reduced tumor growth was observed in mice that received 2 injections (1.1 and 1.3 MBq) of $^{149}$Tb-cm09 (group b, Fig. 4A). One mouse of group b experienced complete tumor regression. In the other 2 mice, KB tumors stopped growing after therapy and started to regrow again several days later.

**TABLE 2**
Biodistribution of $^{161}$Tb-cm09 in KB Tumor–Bearing Female Nude Mice

| | Time after injection (h) | | | | | |
|---|---|---|---|---|---|---|
| Organ | 1 | 4 | 24 | 48 | 96 | 168 |
| Blood | 11.2 ± 1.1 | 6.1 ± 0.3 | 1.5 ± 0.1 | 0.72 ± 0.18 | 0.16 ± 0.01 | 0.04 ± 0.01 |
| Lung | 6.3 ± 0.5 | 4.1 ± 0.3 | 1.6 ± 0.1 | 1.0 ± 0.3 | 0.54 ± 0.08 | 0.21 ± 0.06 |
| Spleen | 2.5 ± 0.5 | 1.8 ± 0.2 | 0.99 ± 0.19 | 0.86 ± 0.09 | 0.71 ± 0.03 | 0.44 ± 0.11 |
| Kidneys | 20.5 ± 2.7 | 27.5 ± 1.1 | 27.8 ± 5.0 | 24.5 ± 1.6 | 15.5 ± 3.2 | 7.4 ± 1.7 |
| Stomach | 2.6 ± 0.5 | 2.1 ± 0.3 | 0.99 ± 0.37 | 0.65 ± 0.19 | 0.39 ± 0.08 | 0.17 ± 0.05 |
| Intestines | 1.9 ± 0.3 | 1.2 ± 0.2 | 0.31 ± 0.05 | 0.34 ± 0.06 | 0.13 ± 0.02 | 0.06 ± 0.03 |
| Liver | 5.5 ± 0.3 | 5.1 ± 0.6 | 3.8 ± 0.7 | 2.3 ± 0.4 | 1.6 ± 0.2 | 0.86 ± 0.16 |
| Salivary glands | 9.9 ± 1.1 | 9.3 ± 0.8 | 5.8 ± 1.3 | 3.9 ± 0.6 | 2.6 ± 0.1 | 1.3 ± 0.5 |
| Muscle | 1.8 ± 0.1 | 1.9 ± 0.2 | 1.3 ± 0.1 | 0.70 ± 0.03 | 0.45 ± 0.06 | 0.16 ± 0.08 |
| Bone | 2.0 ± 0.2 | 1.8 ± 0.1 | 1.3 ± 0.3 | 0.56 ± 0.23 | 0.46 ± 0.04 | 0.22 ± 0.01 |
| Tumor | 14.1 ± 0.6 | 23.8 ± 2.5 | 22.0 ± 4.4 | 18.5 ± 1.8 | 10.3 ± 1.8 | 5.7 ± 1.9 |
| Tumor to blood | 1.2 ± 0.1 | 3.9 ± 0.3 | 14.3 ± 2.0 | 26.8 ± 6.5 | 64.7 ± 8.4 | 129.4 ± 18.0 |
| Tumor to liver | 2.6 ± 0.2 | 4.7 ± 0.5 | 5.9 ± 0.6 | 8.1 ± 1.7 | 6.5 ± 1.7 | 6.5 ± 1.2 |
| Tumor to kidney | 0.68 ± 0.07 | 0.87 ± 0.12 | 0.79 ± 0.05 | 0.75 ± 0.04 | 0.70 ± 0.09 | 0.76 ± 0.12 |



UH & EURATOM Exhibit 2041-005
Fusion v. Universität Heidelberg, et al.
IPR2023-00551

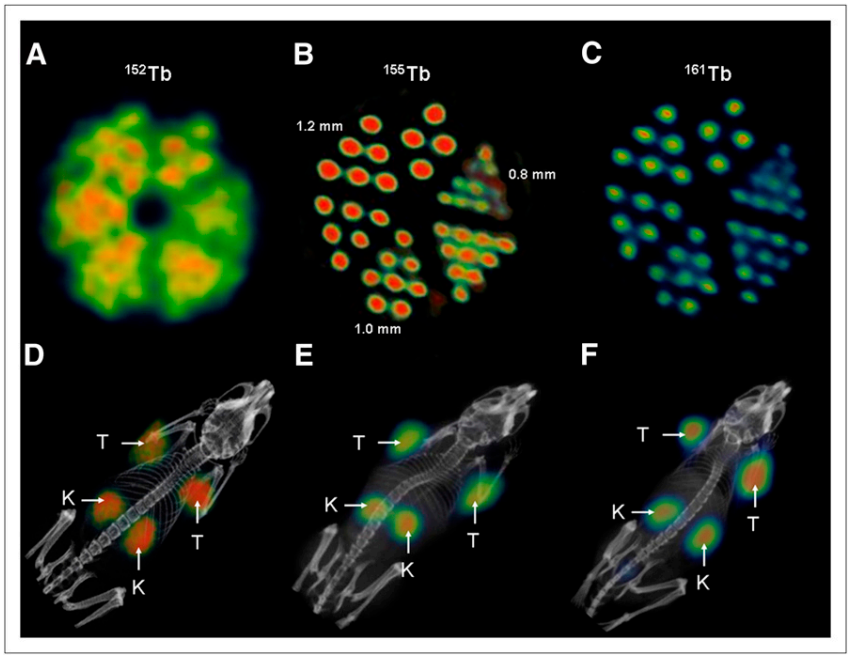


**FIGURE 3.** (A) PET image of Derenzo phantoms (~1.9 MBq of $^{152}$Tb). (B and C) SPECT images of Derenzo phantoms (~0.6 MBq of $^{155}$Tb and ~50 MBq of $^{161}$Tb, respectively). (D) PET/CT image of KB tumor–bearing mouse at 24 h after injection of $^{152}$Tb-cm09, (E and F) SPECT/CT images of KB tumor–bearing mice at 24 h after injection of $^{155}$Tb-cm09 (E) and $^{161}$Tb-cm09 (F). K = kidney; T = KB tumor xenograft.

In the case of $^{161}$Tb-cm09, tumor growth was clearly reduced in all mice, compared with the untreated controls (group c, Fig. 4B). Only 1 mouse (d4) experienced tumor escape, whereas the other 4 mice showed complete tumor remission.

In both groups of mice treated with either $^{149}$Tb-cm09 (group b) or $^{161}$Tb-cm09 (group d), a slight body weight loss was observed within the first 6–7 d after therapy, compared with continuous weight gain in untreated control mice (groups a and c) (Figs. 5A and 5B). However, none of the mice reached the endpoint criterion. In contrast, about 2 wk after the start of the therapy, the averaged relative body weight reached the level of the body weight at day 0.

In the α-therapy study, the average survival of control mice (group a) was 32 d. The animals (a1–a3) had to be euthanized at days 28, 32, and 36 after therapy because the tumor size criterion had been exceeded (Fig. 5C). In the case of mice treated with $^{149}$Tb-cm09 (group b), the survival time was significantly prolonged ($P < 0.05$). The animals (b1 and b2) had to be euthanized at days 42 and 56 after therapy because of tumor size. Mouse b3 showed complete remission and hence was still alive without detectable tumors at the end of the study at day 56 (Fig. 5C).

In the $\beta^-$ therapy study, the average survival of control mice (group c) was 28 d. The animals (c1–c5) had to be euthanized between day 24 and day 30 because of oversized tumors (Fig. 5D). Again, a significantly longer survival time ($P < 0.005$) was observed in mice treated with $^{161}$Tb-cm09 (group d). Only 1 mouse (d4) had to be euthanized because of a large tumor burden at day 38. The remaining 4 mice of group d (d1–d3 and d5) experienced complete tumor regression, and thus all of them were alive at the end of the study at day 56.

## DISCUSSION

The $\beta^-$- and Auger-electron emitter $^{161}$Tb is an interesting alternative to $^{177}$Lu, which is in routine clinical use (e.g., $^{177}$Lu-DOTATATE (*3,12,13*)). The production of the novel therapeutic $\beta^-$-emitter $^{161}$Tb has recently been reported by

**TABLE 3**
Set-up of α-Therapy Study Using $^{149}$Tb-cm09 and $\beta^-$-Therapy Study Using $^{161}$Tb-cm09 in KB Tumor–Bearing Nude Mice

| Therapy study | Mouse identification | Test agent | Injection protocol | Amount of radioactivity |
|---|---|---|---|---|
| α | | | | |
| Control group | a1, a2, a3 | PBS | Days 0 and 4 | — |
| Treated group | b1, b2, b3 | $^{149}$Tb-cm09 | Days 0 and 4 | 1.1 and 1.3 MBq |
| $\beta^-$ | | | | |
| Control group | c1, c2, c3, c4, c5 | PBS | Day 0 | — |
| Treated group | d1, d2, d3, d4, d5 | $^{161}$Tb-cm09 | Day 0 | 11 MBq |

*Irradiation of even highly enriched $^{152}$Gd targets would presumably result in only moderate yield and quality of $^{149}$Tb because of concomitant production of side products ($^{150}$Tb, $^{151}$Tb) and $^{149m}$Tb.



UH & EURATOM Exhibit 2041-006
Fusion v. Universität Heidelberg, et al.
IPR2023-00551

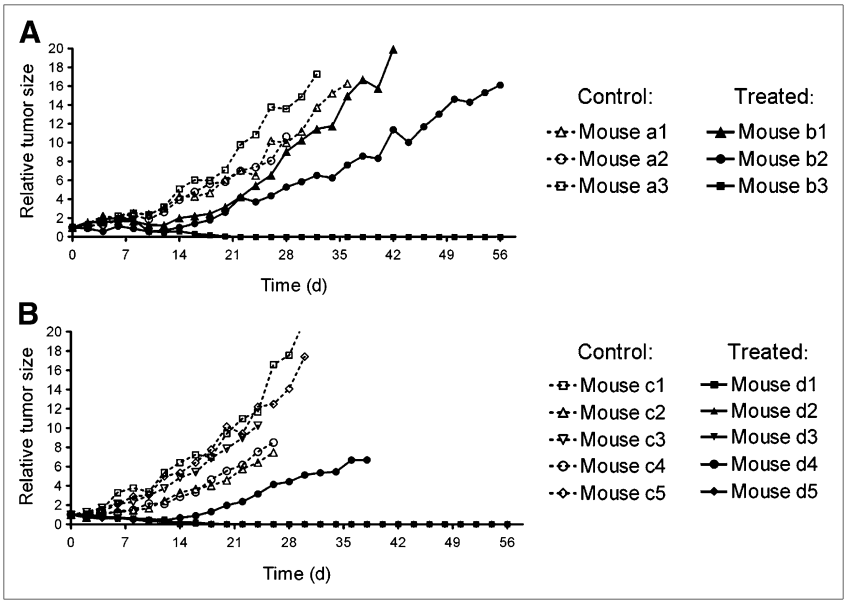


**FIGURE 4.** Graphs representing average tumor size of each mouse of groups a–c relative to averaged tumor size determined at day 0. (A) $^{149}$Tb-cm09 therapy study: mice a1–a3 (untreated control mice) and mice b1–b3 (mice treated with 2.4 MBq of $^{149}$Tb). (B) $^{161}$Tb-cm09 therapy study: mice c1–c5 (untreated control mice) and mice d1–d5 (mice treated with 11 MBq of $^{161}$Tb).

our group (*3*). The radionuclide is obtained by irradiation of enriched $^{160}$Gd targets with neutrons. After radiochemical isolation, $^{161}$Tb is available in a no-carrier-added form that is useful for the radiolabeling of biomolecules at high specific activities. Because of its ease of production, the specific activities achievable, the emission of considerable amounts of conversion and Auger electrons, and the emission of $\beta^-$-radiation, we propose $^{161}$Tb as a more effective alternative to the widely used $^{177}$Lu (*3,14*). For proof of concept, we are currently conducting comparative therapy studies between $^{161}$Tb- and $^{177}$Lu-radiolabled tumor-targeting molecules.

Neutron-deficient terbium isotopes $^{149}$Tb, $^{152}$Tb, and $^{155}$Tb can also be produced by irradiation of enriched gadolinium targets with protons (*15*). The suitable nuclear reactions for the production of $^{149}$Tb and $^{152}$Tb are $^{152}$Gd(p,4n)$^{149}$Tb* and $^{152}$Gd(p,n)$^{152}$Tb, respectively. The drawback of this strategy is the low enrichment grade (<30%) of commercially available $^{152}$Gd (Supplemental Table 1). The stable gadolinium isotopes of mass numbers between 154 and 160 in the target material would result in the accumulation of terbium radionuclide impurities, which cannot be separated chemically. Therefore, a higher enrichment grade of $^{152}$Gd targets is needed to achieve a high quality of $^{149}$Tb* and $^{152}$Tb, produced by proton irradiations. In contrast, highly enriched $^{155}$Gd (Supplemental Table 1) is commercially available and can be used efficiently as target material for the production of $^{155}$Tb via the $^{155}$Gd(p,n)$^{155}$Tb reaction. An alternative to the production of

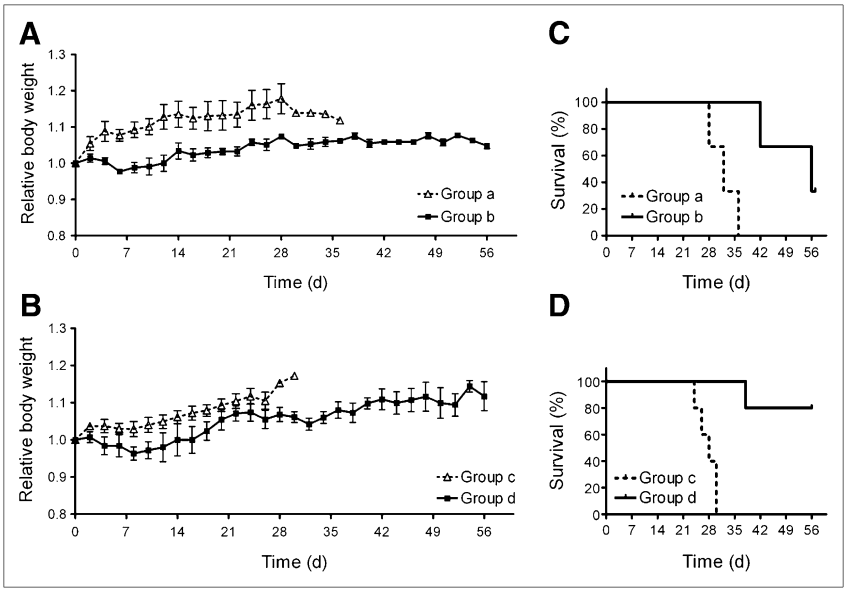


**FIGURE 5.** Graphs representing averaged relative body weight (A and B) and survival curves (C and D) of α-therapy study (A and C) and $\beta^-$-therapy study (B and D). α-therapy: group a (untreated control mice, $n = 3$) and group b (mice treated with $^{149}$Tb-cm09, $n = 3$); $\beta^-$-therapy: group c (untreated control mice, $n = 5$) and group d (mice treated with $^{161}$Tb-cm09, $n = 5$).



UH & EURATOM Exhibit 2041-007
Fusion v. Universität Heidelberg, et al.
IPR2023-00551

$^{149}$Tb and $^{152}$Tb using protons would be heavy ion-induced reactions. These strategies were described and evaluated in detail recently (*2,16*). For the present study, $^{149}$Tb, $^{152}$Tb, and $^{155}$Tb were produced by high-energy proton-induced spallation of tantalum, followed by online mass separation at ISOLDE facility CERN. This is a universal production method, which is also applicable to neutron-deficient lanthanides. Thus, batches of $^{149}$Tb, $^{152}$Tb, and $^{155}$Tb of up to 1 GBq are producible at ISOLDE. This method is presumably not an option for large-scale production of these isotopes. Nevertheless, we believe there is extreme value in proving the suitability of these novel radionuclides for future biomedical use. The establishment of a method for large-scale production with high-power proton accelerators is under investigation.

The application of $^{149}$Tb for targeted α-therapy has been proposed recently (*17,18*). So far, there is only a single preclinical therapy study reported in the literature, in which $^{149}$Tb has been successfully used for α-therapy in a leukemia mouse model with an antibody as a targeting agent (*1*). The present work demonstrated for the first time the successful therapeutic application of $^{161}$Tb in vivo. Furthermore, we were able to perform both $^{149}$Tb- and $^{161}$Tb-based α- and $\beta^-$-radionuclide therapy in the same tumor mouse model, using the same targeting agent, namely a folate-based DOTA conjugate (cm09).

The amount of $^{149}$Tb-cm09 available from 2 production cycles at ISOLDE was applied to a group of 3 mice in 2 fractions (1.1 and 1.3 MBq/mouse). The amount of $^{161}$Tb-cm09 (11 MBq/mouse) was adjusted to obtain roughly the same equivalent adsorbed dose in tumor xenografts (supplemental data). Considering the different half-lives and biologic efficiencies of α-particles and electrons, we estimated that a 4.5-times-higher radioactivity of $^{161}$Tb than $^{149}$Tb must be injected to reach the same dose.

Tumors of control mice that received only PBS were constantly growing over time until they reached a volume of 1,500 mm$^3$, which was defined as an endpoint criterion and required euthanasia. In contrast, tumor growth was inhibited in mice that received radionuclide therapy through $^{149}$Tb-cm09 or $^{161}$Tb-cm09, and consequently the survival time of treated animals was significantly longer than that of untreated controls. Because of the limited number of test animals that could be included in this pilot study, it would be premature to make final conclusions on the relative anticancer effect of $^{161}$Tb-cm09, compared with $^{149}$Tb-cm09. Using chemically identical radiopharmaceuticals with either an α-particle emission suitable to treat single disseminated tumor cells or a $\beta^-$-particle emission allowing the treatment of larger tumors almost ideally addresses the individual situations in many cancer patients (*19*). The application of $^{149}$Tb and $^{161}$Tb cocktails to optimize efficacy is an intriguing option for these therapeutic isotopes (*19,20*). As a next step, systematic investigations of $^{149}$Tb- and $^{161}$Tb-based α- and $\beta^-$-radionuclide therapy in direct comparative studies will be performed with larger cohorts of animals in our laboratories. The proposed concept may allow for better understanding of biologic response to α- and $\beta^-$-radionuclide therapy because it can be performed in the same in vivo model, using the same targeting agent.

$^{152}$Tb-cm09 and $^{155}$Tb-cm09 allowed excellent visualization of tumor xenografts of mice via small-animal PET and SPECT. On the basis of these findings, it is likely that $^{152}$Tb and $^{155}$Tb would become ideal diagnostic matches for $^{149}$Tb and $^{161}$Tb, providing absolutely identical chemical properties enabling diagnosis, accurate dosimetry, and monitoring of therapy.

## CONCLUSION

This proof-of-concept study is the first report, to our knowledge, on 4 different terbium radioisotopes that have been applied in vivo using the same targeting agent. In a preclinical pilot experiment, we were able to demonstrate the therapeutic effect of the novel radioisotope $^{161}$Tb and directly compare $^{149}$Tb- and $^{161}$Tb-based α- and $\beta^-$-radionuclide therapy. PET and SPECT images were obtained from FR-positive tumor-bearing mice injected with $^{152}$Tb-cm09, $^{155}$Tb-cm09, or $^{161}$Tb-cm09. The concept of this quadruplicate of terbium matches is unique in that it enables the application of chemically and biologically identical radioconjugates for multiple purposes. The clinical value of a matched quadruplet of terbium isotopes requires further, more extensive preclinical studies using other tumor-targeting molecules.

## DISCLOSURE STATEMENT

The costs of publication of this article were defrayed in part by the payment of page charges. Therefore, and solely to indicate this fact, this article is hereby marked "advertisement" in accordance with 18 USC section 1734.


## ACKNOWLEDGMENTS

We thank Dr. Peter Bläuenstein, Dr. Stefanie Krämer, Dr. Adrienne Müller, Josefine Reber, Nadja Romano, and Claudia Keller for technical assistance. We are grateful to the ISOLDE collaboration and the ISOLDE technical team for providing $^{149,152,155}$Tb and to ILL and SINQ for $^{161}$Tb. This project was supported by the Swiss South African Joint Research Program (JRP 12), the Swiss National Science Foundation (Ambizione, grant PZ00P3_121772), and the European Union via the ENSAR project (contract 262010). No other potential conflict of interest relevant to this article was reported.


## REFERENCES


1. Beyer GJ, Miederer M, Vranjes-Duric S, et al. Targeted alpha therapy in vivo: direct evidence for single cancer cell kill using $^{149}$Tb-rituximab. *Eur J Nucl Med Mol Imaging.* 2004;31:547–554.
2. Allen BJ, Goozee G, Sarkar S, Beyer G, Morel C, Byrne AP. Production of terbium-152 by heavy ion reactions and proton induced spallation. *Appl Radiat Isot.* 2001;54:53–58.





**UH & EURATOM Exhibit 2041-008**
**Fusion v. Universität Heidelberg, et al.**
**IPR2023-00551**

3. Lehenberger S, Barkhausen C, Cohrs S, et al. The low-energy beta$^-$ and electron emitter $^{161}$Tb as an alternative to $^{177}$Lu for targeted radionuclide therapy. *Nucl Med Biol.* 2011;38:917–924.
4. Hilgenbrink AR, Low PS. Folate receptor-mediated drug targeting: from therapeutics to diagnostics. *J Pharm Sci.* 2005;94:2135–2146.
5. Low PS, Henne WA, Doorneweerd DD. Discovery and development of folic-acid-based receptor targeting for imaging and therapy of cancer and inflammatory diseases. *Acc Chem Res.* 2008;41:120–129.
6. Müller C, Schibli R. Folic acid conjugates for nuclear imaging of folate receptor-positive cancer. *J Nucl Med.* 2011;52:1–4.
7. Müller C, Struthers H, Winiger C, Zhernosekov K, Schibli R. Novel DOTA conjugate with an albumin binding entity enables the first folic acid targeted $^{177}$Lu-radionuclide tumor therapy in mice. *J Nucl Med.* In press.
8. Köster U, ISOLDE Collaboration. ISOLDE target and ion source chemistry. *Radiochim Acta.* 2001;89:749–756.
9. Müller C, Mindt TL, de Jong M, Schibli R. Evaluation of a novel radiofolate in tumour-bearing mice: promising prospects for folate-based radionuclide therapy. *Eur J Nucl Med Mol Imaging.* 2009;36:938–946.
10. Ladino CA, Chari RVJ, Bourret LA, Kedersha NL, Goldmacher VS. Folate-maytansinoids: target-selective drugs of low molecular weight. *Int J Cancer.* 1997;73:859–864.
11. Mathias CJ, Wang S, Lee RJ, Waters DJ, Low PS, Green MA. Tumor-selective radiopharmaceutical targeting via receptor-mediated endocytosis of gallium-67-deferoxamine-folate. *J Nucl Med.* 1996;37:1003–1008.
12. Kwekkeboom DJ, de Herder WW, Kam BL, et al. Treatment with the radiolabeled somatostatin analog [$^{177}$Lu-DOTA$^0$,Tyr$^3$]octreotate: toxicity, efficacy, and survival. *J Clin Oncol.* 2008;26:2124–2130.
13. de Jong M, Breeman WA, Bernard BF, et al. Evaluation in vitro and in rats of $^{161}$Tb-DTPA-octreotide, a somatostatin analogue with potential for intraoperative scanning and radiotherapy. *Eur J Nucl Med.* 1995;22:608–616.
14. Uusijärvi H, Bernhardt P, Rosch F, Maecke HR, Forssell-Aronsson E. Electron- and positron-emitting radiolanthanides for therapy: aspects of dosimetry and production. *J Nucl Med.* 2006;47:807–814.
15. Vermeulen C, Steyn GF, Szelecsenyi F, et al. Cross sections of proton-induced reactions on $^{nat}$Gd with special emphasis on the production possibilities of $^{152}$Tb and $^{155}$Tb. *Nucl Instrum Methods Phys Res B.* 2012;275:24–32.
16. Beyer GJ, Comor JJ, Dakovic M, et al. Production routes of the alpha emitting $^{149}$Tb for medical application. *Radiochim Acta.* 2002;90:247–252.
17. Rizvi SM, Allen BJ, Tian Z, Goozee G, Sarkar S. In vitro and preclinical studies of targeted alpha therapy (TAT) for colorectal cancer. *Colorectal Dis.* 2001;3:345–353.
18. Allen BJ, Rizvi S, Li Y, Tian Z, Ranson M. In vitro and preclinical targeted alpha therapy for melanoma, breast, prostate and colorectal cancers. *Crit Rev Oncol Hematol.* 2001;39:139–146.
19. Carlsson J, Forssell Aronsson E, Hietala SO, Stigbrand T, Tennvall J. Tumour therapy with radionuclides: assessment of progress and problems. *Radiother Oncol.* 2003;66:107–117.
20. Zweit J. Radionuclides and carrier molecules for therapy. *Phys Med Biol.* 1996;41:1905–1914.



**UH & EURATOM Exhibit 2041-009**
**Fusion v. Universität Heidelberg, et al.**
**IPR2023-00551**